PNAS RESEARCH ARTICLE | NEUROSCIENCE

The ISR downstream target ATF4 represses long-term memory in a cell type–specific manner

Niaz Mahmood[a,b,1,2], Jung-Hyun Choi[a,b,1], Pei You Wu[c], Sean W. Dooling[d], Trent A. Watkins[d], Ziying Huang[a,b], Jesse Lipman[a,b], Hanjie Zhao[a,b], Anqi Yang[a,b], Jake Silversmith[a,b], Yanis Inglebert[c,e], Constantinos Koumenis[f], Vijendra Sharma[g], Jean-Claude Lacaille[e], Wayne S. Sossin[h], Arkady Khoutorsky[i,j], R. Anne McKinney[c], Mauro Costa-Mattioli[d,k,l,2], and Nahum Sonenberg[a,b,2]

Affiliations are included on p. 7.

Contributed by Nahum Sonenberg; received April 14, 2024; accepted June 25, 2024; reviewed by Clive Bramham and Satoshi Kida

The integrated stress response (ISR), a pivotal protein homeostasis network, plays a critical role in the formation of long-term memory (LTM). The precise mechanism by which the ISR controls LTM is not well understood. Here, we report insights into how the ISR modulates the mnemonic process by using targeted deletion of the activating transcription factor 4 (ATF4), a key downstream effector of the ISR, in various neuronal and non-neuronal cell types. We found that the removal of ATF4 from forebrain excitatory neurons (but not from inhibitory neurons, cholinergic neurons, or astrocytes) enhances LTM formation. Furthermore, the deletion of ATF4 in excitatory neurons lowers the threshold for the induction of long-term potentiation, a cellular model for LTM. Transcriptomic and proteomic analyses revealed that ATF4 deletion in excitatory neurons leads to upregulation of components of oxidative phosphorylation pathways, which are critical for ATP production. Thus, we conclude that ATF4 functions as a memory repressor selectively within excitatory neurons.

integrated stress response | learning and memory | synaptic plasticity | protein synthesis

Significance

The activation of the integrated stress response (ISR) underlies memory deficits in various cognitive disorders, but how ISR regulates long-term memory (LTM) remains largely unknown. Here, we show that deleting activating transcription factor 4 (ATF4), a downstream target of ISR, in excitatory neurons but not in inhibitory and cholinergic neurons or astrocytes bolsters LTM-associated behaviors. Therefore, in excitatory neurons, ATF4 plays a major role in regulating ISR-mediated mnemonic processes.

The integrated stress response (ISR) is a phylogenetically conserved signaling network that maintains cellular proteostasis by tuning protein synthesis (1). A large body of evidence documents the ISR as a central molecular switch that regulates long-term memory (LTM) formation (1, 2). Genetic or pharmacological suppression of the ISR enhances the formation of LTM (3–6). In contrast, ISR activation, which leads to global reduction in protein synthesis but increase in the translation of activating transcription factor 4 (ATF4) (7) (Fig. 1*A*), impairs LTM (3, 8–10). However, it remains to be determined whether ATF4 serves as the primary downstream effector of ISR during the formation of LTM.

ATF4 belongs to the basic leucine zipper domain (bZip) family of transcription factors and functions in a context-dependent manner either as a transcriptional repressor or activator (11). ISR activation impaired protein synthesis–dependent long-term potentiation (LTP) in hippocampal slices from control (wild type; WT) mice but not in ATF4-deficient slices (3), suggesting that ATF4 is a major factor driving this process. Moreover, expressing a dominant negative inhibitor of ATF4 [and CCAAT/enhancer-binding proteins (C/EBPs)] in murine forebrain neurons promoted long-term synaptic plasticity and memory formation (12). In contrast to these findings, shRNA-mediated *Atf4* knockdown in the mouse hippocampus impaired synaptic plasticity and LTM (13). It is noteworthy that many of the methods employed to investigate the involvement of ATF4 in the formation of LTM have important limitations as they can potentially a) target other proteins (e.g., C/EBPs) (12) and b) exhibit shRNA-mediated off-target effects (14–16), all of which may confound the interpretation of the results. Moreover, germline deletion of *Atf4* in mice results in defects in ocular, skeletal, and hematopoietic development (17), rendering them unsuitable for studying LTM. In addition, compensatory/adaptive mechanisms could occur when a gene is deleted in the germline (18). To circumvent these shortcomings, we deleted *Atf4* in different cell populations (excitatory neurons, inhibitory interneurons, cholinergic neurons, and astrocytes) to dissect the role of ATF4 in different brain cell types and investigated how it controls LTM. Unexpectedly, our results demonstrate that ATF4 represses the formation of LTM in a cell type–specific manner.

Results

Cell Type–Specific Expression of *Atf4* mRNA in the Mouse Brain. *Atf4* mRNA is ubiquitously expressed in the mouse brain (Allen Mouse Brain Atlas; *SI Appendix*, Fig. S1*A*). To examine *Atf4* levels in distinct cell types in the brain, we performed combined RNA in situ hybridization (ISH; RNAscope) and immunohistochemistry

Author contributions: N.M., M.C.-M., and N.S. designed research; N.M., J.-H.C., P.Y.W., S.W.D., T.A.W., Z.H., J.L., H.Z., A.Y., and J.S. performed research; C.K. and R.A.M. contributed new reagents/analytic tools; N.M., J.-H.C., P.Y.W., S.W.D., Y.I., V.S., J.-C.L., W.S.S., A.K., and R.A.M. analyzed data; J.-H.C. and S.W.D. assisted in editing the manuscript; V.S., J.-C.L., W.S.S., and A.K. conceptual support; R.A.M. supervised the electrophysiology experiment; N.S. obtained funding; and N.M., M.C.-M., and N.S. wrote the paper.

Reviewers: C.B., Universitetet i Bergen; and S.K., University of Tokyo.

Competing interest statement: M.C.-M. and S.W.D. are employees of Altos Labs, Inc. M.C.-M. is a shareholder of Altos Labs, Inc. and Mikrovia, Inc. All other authors do not declare any competing/conflicting interests.

[1]N.M. and J.-H.C. contributed equally to this work.

[2]To whom correspondence may be addressed. Email: niaz.mahmood@mcgill.ca, mcostamattioli@altoslabs.com or nahum.sonenberg@mcgill.ca.

This article contains supporting information online at https://www.pnas.org/lookup/suppl/doi:10.1073/pnas.2407472121/-/DCSupplemental.

Published July 24, 2024.

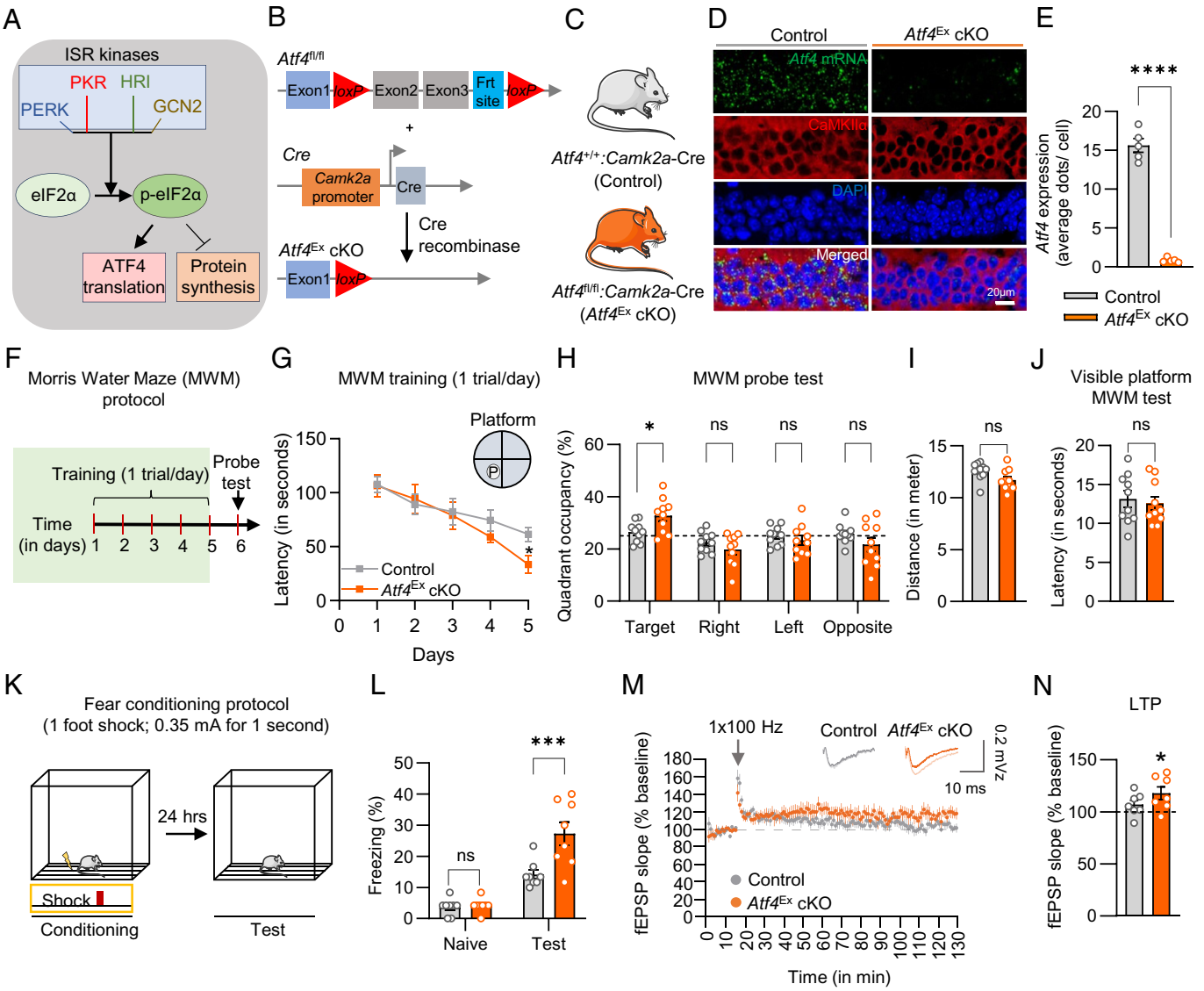

Fig. 1. ATF4 deletion in excitatory neurons facilitates LTM formation. (*A*) Schematic of the ISR pathway. The central component of the ISR, eIF2α, is phosphorylated by four dedicated ISR kinases, which leads to a decrease in global protein synthesis but a paradoxical increase in translation of the *Atf4* mRNA. (*B*) The breeding strategy used to generate forebrain excitatory neuron-specific *Atf4* knockout mice. (*C*) Control (*Atf4*$^{+/+}$:*Camk2a*-Cre) and mice in which ATF4 is deleted in excitatory neurons (*Atf4*$^{fl/fl}$:*Camk2a*-Cre; here defined as *Atf4*^{Ex} cKO). (*D*) Combined ISH/IHC shows selective deletion of *Atf4* (green dots) in the CaMKIIα-positive excitatory neurons (depicted by "red" staining) in the CA1 region of *Atf4*^{Ex} cKO mice compared to the control group. (*E*) Quantification of *Atf4* mRNA levels in control and *Atf4*^{Ex} cKO mice (t = 16.55, degrees of freedom (df) = 4.202, n = 5/group, $P < 0.0001$, unpaired t test with Welch's correction; each point in the graph represents means per mouse). (*F*) Protocol for weak MWM test. (*G* and *H*) Enhanced spatial LTM acquisition in *Atf4*^{Ex} cKO mice (Day 5: n = 10/group, P = 0.0471, two-way ANOVA with Tukey's post hoc comparisons) and preference for the target quadrant on the probe test under a weak training paradigm (n = 10/group, P = 0.0130, two-way ANOVA with Tukey's post hoc comparisons). The *Atf4*^{Ex} cKO mice spent significantly more time than the baseline by a one-sample t test (P = 0.0048 for *Atf4*^{Ex} cKO and P = 0.2667 for control mice), indicating that weak training was sufficient to form an LTM. (*I*) The swimming distances of the two genotypes were comparable (mean distance for control: 12.56 ± 0.25 m and *Atf4*^{Ex} cKO: 11.70 ± 0.30 m; t = 2.08, df = 17.51, n = 10/group, P = 0.0525, unpaired t test with Welch's correction). (*J*) The time required to find the visible platform was similar between control and *Atf4*^{Ex} cKO mice (t = 0.4238, df = 17.66, n = 10/group, P = 0.6769, unpaired t test with Welch's correction). (*K*) Schematic of the weak contextual fear conditioning (CFC) protocol (1-foot shock; 0.35 mA for 1 s). The percentage of freezing was calculated for 5 min 24 h posttraining. (*L*) Long-term contextual fear memory is enhanced in *Atf4*^{Ex} cKO mice compared to the control group (n = 8/group, On test day: P = 0.0003, two-way ANOVA with Bonferroni's post hoc comparisons). (*M*) Time course of normalized synaptic changes induced by high-frequency stimulation (100 Hz for 1 s) in control (n = 7 slices obtained from five mice) and *Atf4*^{Ex} cKO mice (n = 7 slices obtained from six mice). (*N*) Quantification of average LTP recording after stimulation (last 10 min of recording). Average LTP for control = 106.9 ± 4.2 and *Atf4*^{Ex} cKO = 118.1 ± 6.1; the asterisk (*) indicates a significant increase from the baseline 100 as determined by a Wilcoxon test (P = 0.0469). Data are mean ± SEM. *$P < 0.05$, ***$P < 0.001$, ****$P < 0.0001$, n.s. = not significant.

(IHC) on mouse hippocampal sections. This approach was chosen as commercial ATF4 antibodies do not provide reliable IHC signals in mouse brain sections. The combined ISH/IHC revealed that *Atf4* mRNA was coexpressed with markers of various neuronal subtypes, such as calcium/calmodulin-dependent protein kinase type II subunit alpha (CaMKIIα) for excitatory neurons, glutamic acid decarboxylase 67 (GAD67) for inhibitory neurons, and choline acetyltransferase (ChAT) for cholinergic neurons (*SI Appendix*, Fig. S1*B*). However, only a small fraction of *Atf4* mRNAs colocalized with glial fibrillary acidic protein (GFAP) (*SI Appendix*, Fig. S1*B*), indicating low basal ATF4 expression in the astrocytes, in accordance with previous reports (19, 20).

Deletion of ATF4 in Forebrain Excitatory Neurons Leads to Enhanced LTM. To study the role of ATF4 in LTM formation in forebrain excitatory neurons, which are critically required for this process (21), we crossed *Atf4*$^{fl/fl}$ mice with *Camk2a*-Cre mice that express Cre postnatally in excitatory forebrain neurons (22) to generate cell type-specific knockout (*Atf4*$^{fl/fl}$:*Camk2a*-Cre;

hereafter denoted *Atf4*^{Ex} cKO) and control (*Atf4*$^{+/+}$*:Camk2a*-Cre) mice, respectively (Fig. 1 *B* and *C*). The selective deletion of *Atf4* in excitatory neurons was confirmed by combined ISH/IHC (Fig. 1 *D* and *E*).

We first examined spatial LTM using the Morris water maze (MWM) test, in which mice use visual cues to find a hidden platform in a circular pool (23). We studied LTM as it requires protein synthesis which is controlled by ISR. Previous studies demonstrated that ISR inhibition facilitates spatial LTM formation under a weak training paradigm (one training session per day for 5 to 6 d; Fig. 1*F*) (3, 4). *Atf4*^{Ex} cKO mice reached the hidden platform significantly faster than control mice (Fig. 1*G*; 45.44 ± 12.19% reduction in escape latency in *Atf4*^{Ex} cKO vs. control on day 5 of training), indicating that ATF4 represses spatial LTM acquisition. Accordingly, unlike control mice, *Atf4*^{Ex} cKO mice spent more time swimming in the target quadrant during the probe test (Fig. 1*H*; *Atf4*^{Ex} cKO and control mice spent 32.76 ± 1.98% and 26.46 ± 1.17% of the total time in the target quadrant, respectively). Additional analysis revealed that *Atf4*^{Ex} cKO mice, but not control mice, spend significantly more time in the target quadrant than chance, further demonstrating that weak training induces LTM in these animals. Notably, the enhanced LTM of *Atf4*^{Ex} cKO mice cannot be attributed to enhanced locomotion since both genotypes swam a similar distance in the circular pool (Fig. 1*I*). Moreover, both control and *Atf4*^{Ex} cKO mice performed comparably in a version of the MWM where the platform was visible to the mice (Fig. 1*J*). Thus, the deletion of *Atf4* in excitatory forebrain neurons promotes spatial LTM.

We also examined spatial LTM using a more robust training paradigm (referred to as the standard MWM test hereafter), consisting of three training trials per day for 5 d (*SI Appendix*, Fig. S2*A*). Both control and *Atf4*^{Ex} cKO mice performed similarly during the LTM acquisition phase (*SI Appendix*, Fig. S2*B*), and no difference was observed in the time spent in the target quadrant during the probe test (*SI Appendix*, Fig. S2*C*). Both control and *Atf4*^{Ex} cKO mice spent significantly more time in the target quadrant than the baseline, indicating the formation of robust LTM in both these groups in the standard MWM protocol. Taken together, these data support the notion that the threshold for forming LTM is lowered in *Atf4*^{Ex} cKO mice.

We next investigated hippocampus-dependent contextual fear memory. In this task, mice receive a foot shock (the unconditioned stimulus; US) in a chosen context (conditioned stimulus; CS). Twenty-four hours after training, mice are exposed to the CS, and their fear response is measured (4). We first used a weak training protocol, which consisted of a mild foot shock (0.35 mA for 1 s) (Fig. 1*K*). Twenty-four hours after training, *Atf4*^{Ex} cKO froze more (~1.9-fold increase) than control mice (Fig. 1*L*), demonstrating enhanced contextual LTM. The freezing behavior of *Atf4*^{Ex} cKO mice was also increased (1.5-fold) when measured 24 h after a stronger training protocol (two shocks of 0.7 mA for 2 s) (*SI Appendix*, Fig. S2 *D* and *E*). No anxiety-like behavior or locomotor alterations were observed in *Atf4*^{Ex} cKO mice (*SI Appendix*, Fig. S2 *F–K*). Thus, long-term fear memory is facilitated in mice lacking ATF4 in forebrain excitatory neurons.

Given that *Atf4*^{Ex} cKO mice exhibited enhanced LTM, we next studied hippocampal LTP, a cellular model underlying LTM formation (24). A single train of high-frequency stimulation (1 × HFS) of the Schaffer collateral pathway elicited a long-lasting LTP only in slices from *Atf4*^{Ex} cKO mice (Fig. 1 *M* and *N*) demonstrating that deletion of ATF4 in forebrain excitatory neurons lowered the threshold for LTP. Therefore, consistent with the genetic inhibition of ISR (5), deletion of *Atf4* in the forebrain excitatory neurons bolsters synaptic plasticity and LTM formation.

Deletion of ATF4 in Inhibitory Neurons, Cholinergic Neurons, or Astrocytes Fails to Enhance LTM. GABAergic inhibitory neurons play a critical role in LTM formation by regulating the activity of excitatory neurons (25). Astrocytes are believed to play a key role in LTM by modulating synaptic functions (26, 27). Genetic inhibition of the ISR in either GABAergic neurons or astrocytes facilitates LTM formation (5, 28). If ATF4 is the major effector of the ISR in inhibitory neurons and astrocytes, it is conceivable that deletion of the *Atf4* gene in these cell types should lead to an enhanced LTM phenotype similar to that of excitatory neurons. To this end, we deleted *Atf4* in inhibitory neurons by crossing *Atf4*$^{fl/fl}$ with mice expressing Cre recombinase under the glutamic-acid decarboxylase 2 (*Gad2*) promoter to generate GABAergic-specific *Atf4* knockout (*Atf4*$^{fl/fl}$*:Gad2*-Cre; hereafter denoted as *Atf4*^{In} cKO) and control (*Atf4*$^{+/+}$*:Gad2*-Cre) mice (Fig. 2*A*). To delete *Atf4* in astrocytes, *Atf4*$^{fl/fl}$ and *Gfap*-Cre mice were cross-bred to obtain astrocyte-specific *Atf4* knockout (*Atf4*$^{fl/fl}$*:Gfap*-Cre; hereafter denoted as *Atf4*^{Astro} cKO) and control (*Atf4*$^{+/+}$*:Gfap*-Cre) mice (Fig. 3*A*). Combined ISH/IHC confirmed that *Atf4* was selectively deleted from GABAergic inhibitory neurons in *Atf4*^{In} cKO (Fig. 2 *B* and *C*) and GFAP-expressing astrocytes in *Atf4*^{Astro} cKO mice (Fig. 3 *B* and *C*).

Strikingly, deletion of the *Atf4* gene from either inhibitory neurons or astrocytes failed to facilitate LTM upon weak MWM (Fig. 2 *D* and *E* for inhibitory neurons and Fig. 3 *D* and *E* for astrocytes) and CFC paradigms (Figs. 2*G* and 3*G* for inhibitory neurons and astrocytes, respectively). Moreover, both genotypes behaved similarly in the standard version of the MWM (*SI Appendix*, Fig. S3 *A* and *B* for inhibitory neurons and *SI Appendix*, Fig. S4 *A* and *B* for astrocytes) or CFC (*SI Appendix*, Fig. S3*C* for inhibitory neurons and *SI Appendix*, Fig. S4*C* for astrocytes). No visual or anxiety-related behavioral abnormalities were observed upon ATF4 deletion in inhibitory neurons or astrocytes (for inhibitory neurons: Fig. 2*F* and *SI Appendix*, Fig. S3 *D–H*; for astrocytes: Fig. 3*F* and *SI Appendix*, Fig. S4 *D–H*). Thus, deletion of ATF4 from inhibitory neurons or astrocytes fails to facilitate LTM.

Finally, regulation of the ISR in cholinergic neurons is also important for LTM formation (29). To study the effects of selective inhibition of the ISR in cholinergic neurons on contextual LTM formation, we crossed *Eif2s1*$^{A/A}$;ftg mice, which allow for cell type–specific mutation of the phosphorylation site at serine 51 in the alpha subunit of eukaryotic translation initiation factor 2 (eIF2) to alanine (S51A) and inhibition of ISR signaling (30, 31), with mice expressing Cre recombinase under the choline acetyltransferase (*ChAT*) promoter (*Eif2s1*^{Chol} cKI) (*SI Appendix*, Fig. S5 *A* and *B*). ISR inhibition in cholinergic neurons facilitated LTM formation, as determined by increased freezing 24 h after a weak fear conditioning training (*SI Appendix*, Fig. S5*E*). To investigate whether memory enhancement as a consequence of ISR inhibition was mediated via ATF4, we generated mice in which ATF4 is deleted in cholinergic neurons, by crossing *Atf4*$^{fl/fl}$ mice and *ChAT*-Cre mice (*Atf4*^{Chol} cKO) (*SI Appendix*, Fig. S5 *C* and *D*). In contrast to the *Eif2s1*^{Chol} cKI mice, the *Atf4*^{Chol} cKO mice performed similarly to control mice in the CFC test (*SI Appendix*, Fig. S5*F*). Thus, the enhanced LTM caused by inhibition of the ISR in cholinergic neurons is ATF4-independent. Taken together, our results show that deletion of *Atf4* solely in excitatory neurons facilitates LTM formation, which supports the notion that ATF4 represses LTM in a cell type–specific manner.

ATF4 Deletion in Excitatory Neurons Engenders Enhanced Expression of Proteins Involved in Oxidative Phosphorylation. To gain insight into the molecular mechanism underlying the enhanced LTM in mice lacking ATF4 in excitatory neurons, we conducted RNA sequencing (RNA-Seq) on the hippocampus

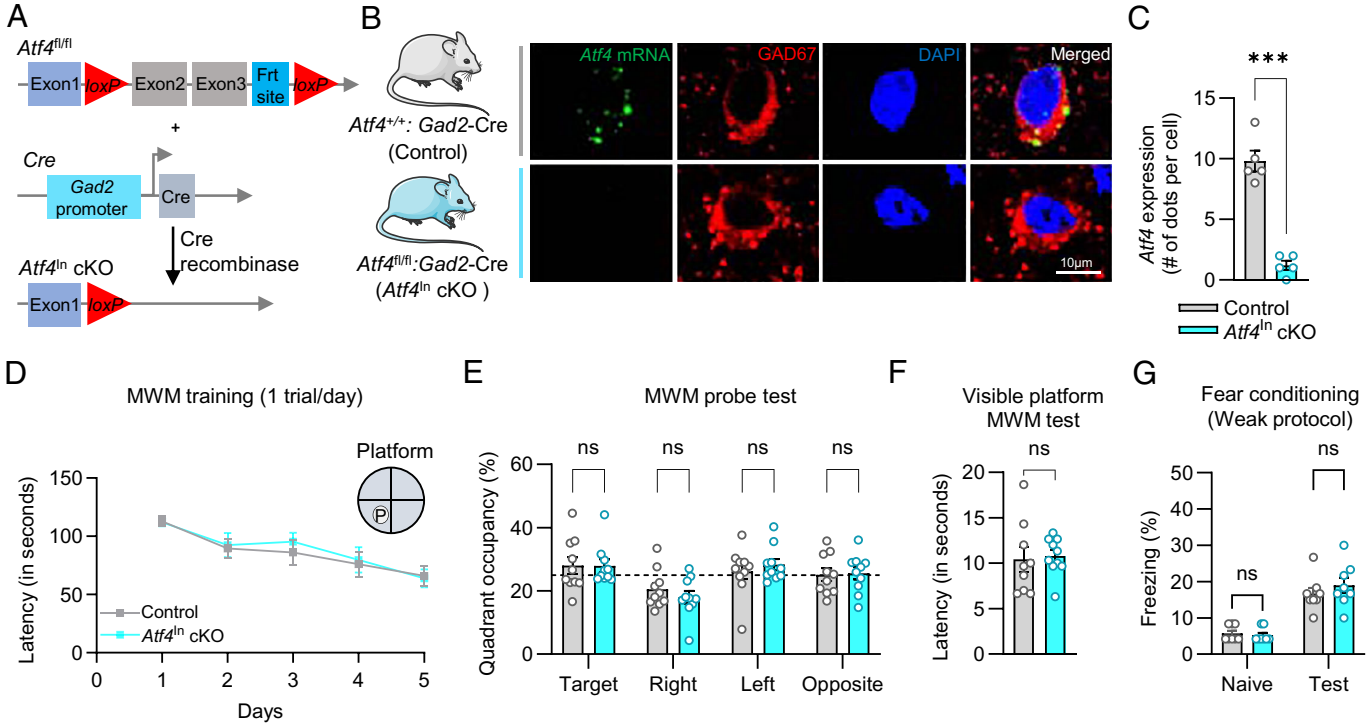

Fig. 2. Deletion of *Atf4* in inhibitory neurons has no effect on LTM formation. (*A*) Schematic of the breeding strategy used to generate inhibitory neuron-specific *Atf4* knockout mice. (*B*) Diagram of the two genotypes of mice *Atf4*$^{+/+}$:*Gad2*-Cre (control) and *Atf4*$^{fl/fl}$:*Gad2*-Cre (*Atf4*^{In} cKO) used in experiments. Combined ISH/IHC showing selective deletion of *Atf4* (green dots) in the GAD67-positive inhibitory neurons (depicted by red staining) of *Atf4*^{In} cKO mice compared to the control group. (*C*) Quantitation of *Atf4* mRNA levels in control and *Atf4*^{In} cKO mice (t = 9.168, df = 5.461, n = 5/group, P = 0.0002, unpaired t test with Welch's correction; each point in the graph represents means per mouse). (*D* and *E*) Deletion of *Atf4* in the inhibitory neurons does not affect memory acquisition, and mice from both genotypes showed similar preference for the target quadrant on the probe test (n = 10/group, P = 0.9786, two-way ANOVA, two-way ANOVA with Tukey's post hoc comparisons). The control and *Atf4*^{In} cKO mice did not spend significantly more time in the target quadrant than the baseline (one-sample t test, P = 0.1357 for control and P = 0.1714 for *Atf4*^{In} cKO), indicating that the weak training was insufficient to induce a robust LTM in both groups. (*F*) Latency to find the visible platform is similar between control and *Atf4*^{In} cKO mice (t = 0.2631, df = 11.67, n = 9 for control and n = 10 for the *Atf4*^{In} group, P = 0.7971, unpaired t test with Welch's correction). (*G*) Long-term contextual fear memory is similar between control and *Atf4*^{In} cKO mice (n = 8 mice/group, On test day: P = 0.5449, two-way ANOVA with Bonferroni's post hoc comparisons). Data are mean ± SEM. ***P < 0.001, n.s. = not significant.

from control and *Atf4*^{Ex} cKO mice (*SI Appendix, Methods and Materials*). A total of 110 genes were differentially expressed (DEGs) in the *Atf4*^{Ex} cKO compared to the control group, of which 94 were up-regulated and 16 down-regulated (*SI Appendix*, Fig. S6*A* and Dataset S1). Importantly, 19% of the DEGs (21 out of the 110) contain documented ATF4 binding sites near the transcription start sites (TSSs) (distance up to ±1,000 bp from TSSs) as determined by the list of targets obtained from publicly available human and mouse ATF4 ChIP-Atlas datasets (32) (*SI Appendix*, Fig. S6*B*). ATF4 represses the cAMP response element-binding protein (CREB) (33), a transcription factor involved in LTM formation (34). Indeed, 36 out of the 110 DEGs contain known CREB binding sites (*SI Appendix*, Fig. S6*C*), suggesting that ATF4 deletion derepresses CREB-mediated gene expression in excitatory neurons. Accordingly, phosphorylation of CREB was also increased by 2.8-fold in the hippocampal lysates of *Atf4*^{Ex} cKO mice compared to controls (*SI Appendix*, Fig. S6*D*).

Notably, pathway analyses revealed an upregulation of genes encoding proteins that function in oxidative phosphorylation (OXPHOS) (*SI Appendix*, Fig. S6*E*). qPCR analysis showed an upregulation of several genes of the OXPHOS pathway (*Cox5b, Ndufa13,* and *Ndufb6*) in the hippocampus from *Atf4*^{Ex} cKO compared to control mice (*SI Appendix*, Fig. S6*F*), consistent with previous results (35).

Given the poor correlation between mRNA levels and their encoded proteins in complex biological samples (36, 37), we examined the proteome of the synaptic compartments from control and *Atf4*^{Ex} cKO mice. Sixty-nine synaptic proteins were differentially expressed in the brain of *Atf4*^{Ex} cKO mice, of which 33 were up-regulated and 36 down-regulated (Fig. 4 *A* and *B* and Dataset S2). Homer3 (but not Homer1 or Homer2), a postsynaptic density-associated protein involved in the formation of fear memory (38) was elevated in synaptosome proteomics *Atf4*^{Ex} cKO mice, and validated by western blotting (Fig. 4 *C* and *D*).

Consistent with the RNA-seq analyses, pathway analysis of the synaptic proteome showed an upregulation of proteins involved in OXPHOS in *Atf4*^{Ex} cKO mice (Fig. 4 *E* and *F*). To investigate the link between ATF4 and OXPHOS, primary neurons from WT and *Atf4*^{Ex} cKO embryos were stained with the cell-permeable tetramethylrhodamine ethyl ester (TMRE) dye to measure the mitochondrial membrane potential ($\Delta\Psi m$), a marker of mitochondrial activity and ATP synthesis (39). *Atf4*^{Ex} cKO neurons displayed a twofold increase in TMRE signal compared to the WT neurons (Fig. 4*G*) at 21 d in vitro (DIV21), a time point when CaMKIIα protein is readily expressed in culture (40) and ATF4 is ~80% depleted in the lysates obtained from primary neurons (Fig. 4*H*). Together, we demonstrate that *Atf4* deletion in excitatory neurons results in enhanced expression of OXPHOS pathway proteins, engendering more ATP production to promote neuronal functions underlying LTM formation.

Discussion

The ISR is a pivotal protein network that controls LTM formation across diverse phyla. Convergent and orthogonal studies demonstrated that genetic inhibition of the ISR pathway by either deleting the ISR kinase general control nonderepressible 2 (GCN2) (41) or

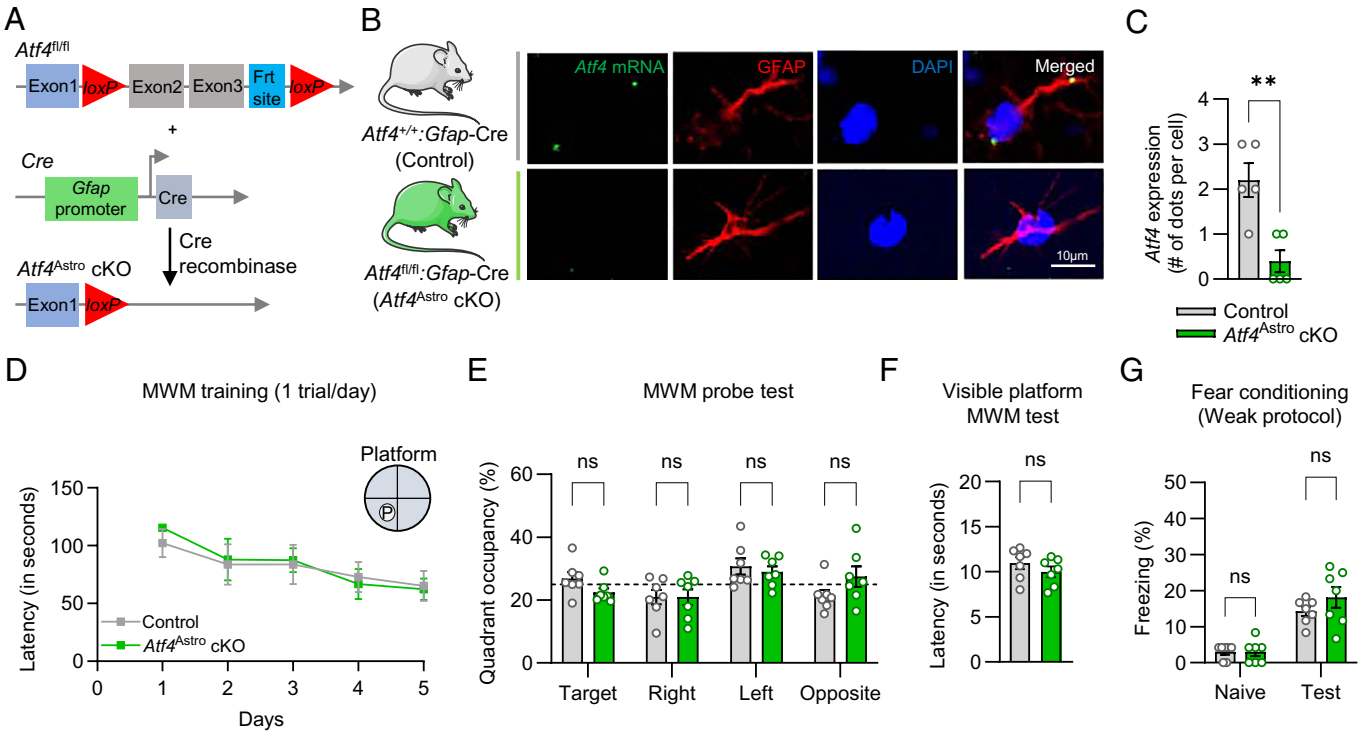

Fig. 3. Deletion of *Atf4* in astrocytes has no effect on LTM formation. (*A*) Schematic of the breeding strategy used to generate astrocyte-specific *Atf4* knockout mice. (*B*) Diagram of the two genotypes of mice *Atf4*$^{+/+}$:*Gfap*-Cre (control) and *Atf4*$^{fl/fl}$:*Gfap*-Cre (*Atf4*^{Astro} cKO) used in experiments. Combined ISH/IHC showing selective deletion of *Atf4* (green dots) in the GFAP-positive astrocytes (depicted by red staining) of *Atf4*^{Astro} cKO mice compared to the control mice. (*C*) Quantitation of *Atf4* mRNA levels in control and *Atf4*^{Astro} cKO mice ($t = 4.025$, df = 6.897, $n = 5$/group, $P = 0.0052$, unpaired t test with Welch's correction; each point in the graph represents means per mouse). (*D* and *E*) Deletion of *Atf4* in the astrocytes does not affect memory acquisition, and mice from both genotypes showed similar preference for the target quadrant on the probe test ($n = 7$/group, $P = 0.1727$, two-way ANOVA with Tukey's post hoc comparisons). The control and *Atf4*^{Astro} cKO mice did not spend significantly more time in the target quadrant than the baseline (one-sample t test, $P = 0.3943$ for control and $P = 0.0868$ for *Atf4*^{Astro} cKO), indicating that the weak training was insufficient to form a robust LTM in both these groups. (*F*) The latency to find the visible platform is similar between the control and *Atf4*^{Astro} cKO ($t = 1.093$, df = 11.83, $n = 7$ mice/group, $P = 0.2960$, unpaired t test with Welch's correction). (*G*) Long-term contextual fear memory is similar between *Atf4*^{Astro} cKO and control mice ($n = 7$ mice/group, On test day: $P = 0.2474$, two-way ANOVA with Bonferroni's post hoc comparisons). Data are mean ± SEM. $^{**}P < 0.01$, n.s. = not significant.

protein kinase R (PKR) (6, 42), or by generating an eIF2α heterozygous knock-in (Ser51Ala) (3) or a cell type–specific eIF2α homozygous knock-in (5, 28), boost LTM formation in mice. In addition, inhibiting the ISR kinases: PKR or protein kinase RNA-like endoplasmic reticulum kinase (PERK) pharmacologically or activating eIF2B, which is converted into an inhibitor of the guanosine diphosphate (GDP) to guanosine triphosphate (GTP) exchange upon ISR activation, with an ISR inhibitor (ISRIB), augments LTM in rodents (4, 6, 42, 43). Conversely, genetic or pharmacological activation of ISR impairs LTM formation (3, 8–10). The ISR bidirectionally controls LTM formation in birds (10). The clinical relevance of the ISR is highlighted by a) the identification of mutations in ISR cardinal genes (encoding eIF2γ and constitutive repressor of eIF2α phosphorylation, CReP) that activate the ISR and are associated with intellectual disabilities in humans (44–47) and b) inhibition of the ISR reverses the LTM decline in several cognitive disorders, including Down syndrome (48) and Alzheimer's disease (49).

A salient feature of the ISR is the enhancement of LTM upon its inhibition in diverse cell types, e.g., excitatory and inhibitory neurons (5) as well as cholinergic neurons (this work) and astrocytes (28). Using a combination of molecular, genetic, behavioral, electrophysiological, and biochemical approaches, we conclusively show that the ISR downstream target ATF4 is an LTM repressor only in excitatory neurons, which comprise the largest percentage (~70 to 80%) of the neuronal cells in the neocortex (50) (key findings are summarized in *SI Appendix*, Fig. S7). The findings that ATF4 is not a general ISR effector that regulates LTM formation across cell types were unexpected. Thus, ISR downstream targets other than ATF4 may repress LTM in other cell types. For instance, oligophrenin-1 (OPHN1), a protein whose synthesis is up-regulated upon mGluR-mediated ISR activation (31), may function as an ISR effector in dopaminergic neurons to control reward-related learning and memory (51, 52). Future studies should aim to elucidate how ISR inhibition in cholinergic neurons, inhibitory neurons, and astrocytes promotes LTM. To this end, one could either use a gene candidate approach (using known ISR targets) or an unbiased genome-wide approach using cell type–specific ribosome profiling. In the latter case, once the ISR downstream targets are identified in different cell types, functional studies are needed to determine their roles during the formation of LTM.

In addition, it is pertinent to examine how ATF4 regulates memory formation in forebrain excitatory neurons. Consistent with the idea that ATF4 is a CREB repressor (3, 33), we have found an increase in CREB-regulated targets in *Atf4*^{Ex} cKO vs. control mice (*SI Appendix*, Fig. S6*C*). Intriguingly, we unveiled that several components of the OXPHOS pathway are up-regulated in *Atf4*^{Ex} cKO mice. Previous studies have shown that inhibition of mitochondrial complex I of the OXPHOS pathway impairs LTP in rodent hippocampal slices (53). Dysregulation of the OXPHOS pathway is also associated with several memory-related disorders. For example, protein components of the OXPHOS pathway are down-regulated in Ts65Dn mice (54, 55), a mouse model of Down's syndrome in which ISR is activated and fear memory is impaired (6). Furthermore, components of OXPHOS such as *Cox5b*, *Ndufa13*, and *Ndufb6*, which exhibit increased expression upon ATF4 deletion in excitatory neurons (*SI Appendix*, Fig. S6*F*), are significantly down-regulated in late-onset Alzheimer's disease (56). Thus, it is conceivable that the

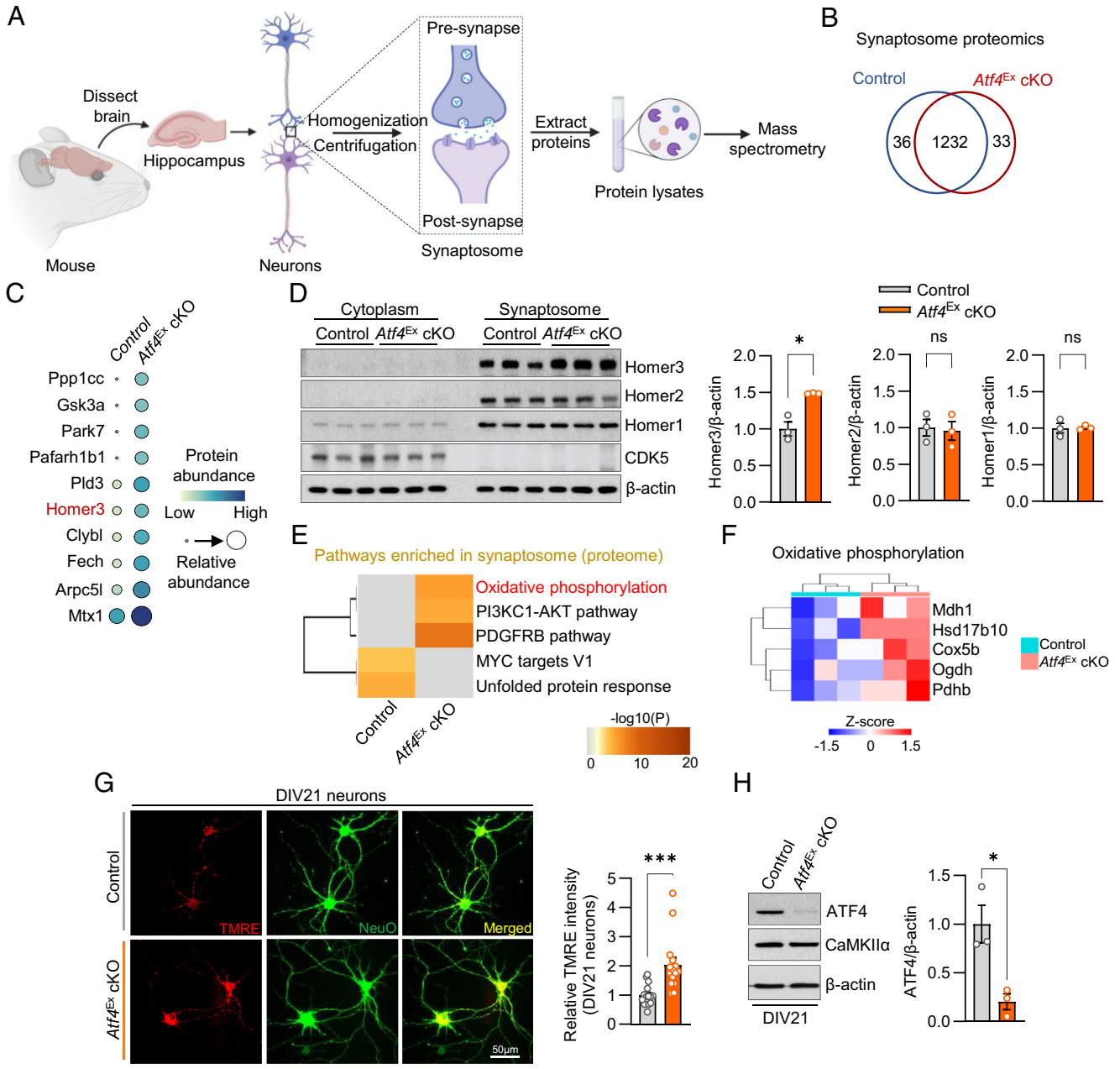

Fig. 4. Selective molecular changes in mice in which *Atf4* is deleted in excitatory neurons. (*A*) Schematic of synaptosome fractionation protocol from the mouse hippocampus (generated using BioRender.com). (*B*) Venn diagram of the common (1,232) and unique (69) protein hits identified in the proteomic analyses of the synaptosome lysates obtained from control and *Atf4*^{Ex} cKO mice. (*C*) Top 10 up-regulated proteins in the synaptosomes of *Atf4*^{Ex} cKO mice (based on foldchange relative to the control mice). (*D*) Western blot from the cytoplasm and synaptosome fractions of control and *Atf4*^{Ex} cKO mice. The blots were probed with antibodies against Homer1, Homer2, and Homer3. β-actin was used as a loading control. Cytoplasmic fraction was run as a control to confirm the purity of the synaptosome fractionation; an antibody against cyclin-dependent kinase 5 (CDK5) was used as a marker of cytoplasmic fraction. The bar graphs in the *Right* panel represent the densitometric quantification of the bands for each protein (n = 3/group; for Homer3: t = 4.953, df = 2.006, P = 0.0382; for Homer2: t = 0.2585, df = 3.939, P = 0.8090; for Homer1: t = 0.1136, df = 2.308, P = 0.9187, unpaired t test with Welch's correction). (*E*) Pathway enrichment analysis of the 69 differentially abundant proteins in the synaptosome of *Atf4*^{Ex} cKO mice. (*F*) Heatmap of the OXPHOS pathway proteins that are up-regulated in the synaptosome of *Atf4*^{Ex} cKO mice. (*G*) Primary hippocampal pyramidal neurons were cultured from the samples obtained from control and *Atf4*^{Ex} cKO mice. The DIV21 neurons were cotreated with TMRE (red) and NeuO (green) and mitochondrial membrane potential (ΔΨm) was determined from the intensity of the signals. Merged images for four different cells per genotype are shown as representatives. Bar graph (on the *Right*) showing the quantification of the TMRE signals. Each dot indicates the intensity of the TMRE signal obtained from a single cell. t = 3.980, df = 18.04, P = 0.0009, unpaired t test with Welch's correction. (*H*) The deletion of *Atf4* in the DIV21 neurons of *Atf4*^{Ex} cKO was confirmed by a western blot using an ATF4 antibody. CaMKIIα expression indicated the activation of Cre in these cells. β-actin was used as a loading control. The bar graph (on the *Right*) shows the densitometric quantification of the ATF4 bands (t = 3.819, df = 2.678, n = 3/group, P = 0.0385, unpaired t test with Welch's correction). Data are mean ± SEM. *P < 0.05, ***P < 0.001, n.s. = not significant.

ISR–ATF4 axis regulates the energy levels required for excitatory synapses to support LTM formation.

Considering that a) LTM formation depends on the intricate interplay of a diverse array of brain cell types and b) ATF4 does not repress LTM via all cell types, it stands to reason that targeting ATF4 across multiple cell types would yield different outcomes compared to targeting it in a single cell type. Accordingly, a prior study employed lentivirus to express a shRNA targeting *Atf4* specifically in the hippocampus, which led to a ~60% reduction in *Atf4* levels and an impairment (not enhancement) in spatial LTM (13). Since non-neuronal cells comprise at least half of the total brain cells (57), this effect could be mediated via non-neuronal cells such as astrocytes, microglia, and oligodendrocytes, which all have roles in memory formation (26, 27, 58, 59). Moreover, a major technical

limitation of RNA interference is the difficulty in achieving efficient and specific knockdown of the target gene in vivo (14). This is particularly challenging in the brain because of the complex neural circuits and diverse cell types involved in LTM formation. Furthermore, the temporal and spatial specificity required to manipulate gene expression either in specific brain areas or time points adds another layer of complexity. For example, even though the MWM is primarily known as a hippocampus-dependent task, impaired connections with other brain regions impact LTM formation (reviewed in ref. 60). It is plausible that targeting ATF4 in one brain region is insufficient to dissect its role in memory. The targeted molecular genetics approach, which we used, selectively deletes *Atf4* in different cell types and mitigates, at least in part, many of the aforementioned limitations. A recent study demonstrated that deletion of *Atf4* in excitatory neurons by injecting Cre-expressing viruses into the brain of $Atf4^{fl/fl}$ mice impairs LTP (61); an immediate explanation of the discrepancy is not clear. Our observation that a single train of high-frequency stimulation is sufficient to induce long-lasting LTP only in slices from $Atf4^{Ex}$ cKO mice is consistent with previous studies with eIF2α knock-in mice (S51A mutant) where both heterozygous (3) and excitatory neuron-specific knock-ins (5) exhibited long-lasting LTP following 1 × HFS, whereas the same stimulation in the control mice induced a short-lasting LTP (5). These results indicate that the inhibition of ISR lowers the threshold for eliciting long-lasting LTP.

Finally, activation of the ISR underlies the cognitive decline associated with a wide range of disorders (44–47). It is therefore imperative to investigate whether targeting *Atf4* in specific cell types could serve as a potential therapeutic option for cognitive disorders.

Methods and Materials

Mice were housed in cages on ventilated racks at a temperature of 20 to 22 °C and a humidity level of approximately 55%, with a standard 12-h light/dark cycle. They had ad libitum access to food (standard rodent chow) and water. At postnatal day 21, mice were separated by sex, weaned, and placed in different cages (2 to 5 mice/cage). All experimental procedures were conducted in compliance with the guidelines established by the animal care committees of McGill University and Baylor College of Medicine. Male mice aged 2- to 5-mo were used for the experiments unless otherwise stated.

Detailed information on experimental procedures is available in *SI Appendix, Materials and Methods*.

Ethics Approval

The animal care and experimental procedures were conducted in compliance with the regulations of the animal care committees of McGill University and Baylor College of Medicine.

Data, Materials, and Software Availability. The data generated in the study data are included in the article and/or *SI Appendix*. Raw sequencing reads are deposited to the Sequence Read Archive (SRA) under the accession PRJNA1134721 (62).

ACKNOWLEDGMENTS. We thank Annie Sylvestre, Annik Lafrance, Isabelle Harvey, and Eva Migon for technical assistance and animal handling. The research was funded by a grant from the Canadian Institutes of Health Research to N.S. (FND-148423). N.M. is supported by a postdoctoral fellowship from the Charlotte and Leo Karassik Foundation. J-H.C. is supported by a Conrad F. Harrington Fellowship.

Author affiliations: [a]Department of Biochemistry, McGill University, Montréal, QC H3A 1A3, Canada; [b]Rosalind and Morris Goodman Cancer Institute, McGill University, Montréal, QC H3A 1A3, Canada; [c]Department of Pharmacology and Therapeutics, McGill University, Montréal, QC H3G 0B1, Canada; [d]Department of Neuroscience, Baylor College of Medicine, Houston, TX 77030; [e]Department of Neurosciences, Center for Interdisciplinary Research on Brain and Learning, Research Group on Neural Signaling and Circuitry, University of Montréal, Montréal, QC H3T1J4, Canada; [f]Department of Radiation Oncology, University of Pennsylvania Perelman School of Medicine, Philadelphia, PA 19104-5156; [g]Department of Biomedical Sciences, University of Windsor, Windsor, ON N9B 3P4, Canada; [h]Department of Neurology and Neurosurgery, Montreal Neurological Institute, McGill University, Montréal, QC H3A 2B4, Canada; [i]Department of Anesthesia and Faculty of Dental Medicine and Oral Health Sciences, McGill University, Montréal, QC H4A3J1, Canada; [j]Alan Edwards Centre for Research on Pain, McGill University, Montréal, QC H3A 2B4, Canada; [k]Memory and Brain Research Center, Baylor College of Medicine, Houston, TX 77030; and [l]Altos Labs Inc., Bay Area Institute of Science, Redwood City, CA 94065

1. M. Costa-Mattioli, P. Walter, The integrated stress response: From mechanism to disease. *Science* **368**, eaat5314 (2020).
2. M. Costa-Mattioli, W. S. Sossin, E. Klann, N. Sonenberg, Translational control of long-lasting synaptic plasticity and memory. *Neuron* **61**, 10–26 (2009).
3. M. Costa-Mattioli *et al.*, eIF2α phosphorylation bidirectionally regulates the switch from short-to long-term synaptic plasticity and memory. *Cell* **129**, 195–206 (2007).
4. C. Sidrauski *et al.*, Pharmacological brake-release of mRNA translation enhances cognitive memory. *eLife* **2**, e00498 (2013).
5. V. Sharma *et al.*, eIF2α controls memory consolidation via excitatory and somatostatin neurons. *Nature* **586**, 412–416 (2020).
6. P. J. Zhu *et al.*, Suppression of PKR promotes network excitability and enhanced cognition by interferon-γ-mediated disinhibition. *Cell* **147**, 1384–1396 (2011).
7. K. M. Vattem, R. C. Wek, Reinitiation involving upstream ORFs regulates *ATF4* mRNA translation in mammalian cells. *Proc. Natl. Acad. Sci. U.S.A.* **101**, 11269–11274 (2004).
8. Z. Jiang *et al.*, eIF2α phosphorylation-dependent translation in CA1 pyramidal cells impairs hippocampal memory consolidation without affecting general translation. *J. Neurosci.* **30**, 2582–2594 (2010).
9. M. Jian *et al.*, eIF2α dephosphorylation in basolateral amygdala mediates reconsolidation of drug memory. *J. Neurosci.* **34**, 10010–10021 (2014).
10. G. Batista, J. L. Johnson, E. Dominguez, M. Costa-Mattioli, J. L. Pena, Translational control of auditory imprinting and structural plasticity by eIF2α. *eLife* **5**, e17197 (2016).
11. K. Ameri, A. L. Harris, Activating transcription factor 4. *Int. J. Biochem. Cell Biol.* **40**, 14–21 (2008).
12. A. Chen *et al.*, Inducible enhancement of memory storage and synaptic plasticity in transgenic mice expressing an inhibitor of ATF4 (CREB-2) and C/EBP proteins. *Neuron* **39**, 655–669 (2003).
13. S. Pasini, C. Corona, J. Liu, L. A. Greene, M. L. Shelanski, Specific downregulation of hippocampal ATF4 reveals a necessary role in synaptic plasticity and memory. *Cell Rep.* **11**, 183–191 (2015).
14. K. Goel, J. E. Ploski, RISC-y business: Limitations of short hairpin RNA-mediated gene silencing in the brain and a discussion of CRISPR/Cas-based alternatives. *Front. Mol. Neurosci.* **15**, 914430 (2022).
15. J. N. Martin *et al.*, Lethal toxicity caused by expression of shRNA in the mouse striatum: Implications for therapeutic design. *Gene Ther.* **18**, 666–673 (2011).
16. A. M. Zimmer, Y. K. Pan, T. Chandrapalan, R. W. M. Kwong, S. F. Perry, Loss-of-function approaches in comparative physiology: Is there a future for knockdown experiments in the era of genome editing? *J. Exp. Biol.* **222**, jeb175737 (2019).
17. H. C. Masuoka, T. M. Townes, Targeted disruption of the activating transcription factor 4 gene results in severe fetal anemia in mice. *Blood* **99**, 736–745 (2002).
18. U. Müller, Ten years of gene targeting: Targeted mouse mutants, from vector design to phenotype analysis. *Mech. Dev.* **82**, 3–21 (1999).
19. R. Liu *et al.*, NOX activation in reactive astrocytes regulates astrocytic LCN2 expression and neurodegeneration. *Cell Death Dis.* **13**, 371 (2022).
20. Y. Wang *et al.*, Mild endoplasmic reticulum stress protects against lipopolysaccharide-induced astrocytic activation and blood–brain barrier hyperpermeability. *Front. Cell Neurosci.* **12**, 222 (2018).
21. M. B. Kennedy, Synaptic signaling in learning and memory. *Cold Spring Harb. Perspect. Biol.* **8**, a016824 (2013).
22. J. Z. Tsien *et al.*, Subregion-and cell type–restricted gene knockout in mouse brain. *Cell* **87**, 1317–1326 (1996).
23. C. V. Vorhees, M. T. Williams, Morris water maze: Procedures for assessing spatial and related forms of learning and memory. *Nat. Protoc.* **1**, 848–858 (2006).
24. T. V. Bliss, G. L. Collingridge, A synaptic model of memory: Long-term potentiation in the hippocampus. *Nature* **361**, 31–39 (1993).
25. L. Topolnik, S. Tamboli, The role of inhibitory circuits in hippocampal memory processing. *Nat. Rev. Neurosci.* **23**, 476–492 (2022).
26. A. Kol *et al.*, Astrocytes contribute to remote memory formation by modulating hippocampal–cortical communication during learning. *Nat. Neurosci.* **23**, 1229–1239 (2020).
27. A. Adamsky *et al.*, Astrocytic activation generates de novo neuronal potentiation and memory enhancement. *Cell* **174**, 59–71.e14 (2018).
28. V. Sharma *et al.*, mRNA translation in astrocytes controls hippocampal long-term synaptic plasticity and memory. *Proc. Natl. Acad. Sci. U.S.A.* **120**, e2308671120 (2023).
29. A. R. Helseth *et al.*, Cholinergic neurons constitutively engage the ISR for dopamine modulation and skill learning in mice. *Science* **372**, eabe1931 (2021).
30. S. H. Back *et al.*, Translation attenuation through eIF2alpha phosphorylation prevents oxidative stress and maintains the differentiated state in beta cells. *Cell Metab.* **10**, 13–26 (2009).
31. G. V. Di Prisco *et al.*, Translational control of mGluR-dependent long-term depression and object-place learning by eIF2α. *Nat. Neurosci.* **17**, 1073–1082 (2014).
32. Z. Zou, T. Ohta, F. Miura, S. Oki, ChIP-Atlas 2021 update: A data-mining suite for exploring epigenomic landscapes by fully integrating ChIP-seq, ATAC-seq and Bisulfite-seq data. *Nucleic Acids Res.* **50**, W175–W182 (2022).
33. D. Bartsch *et al.*, Aplysia CREB2 represses long-term facilitation: Relief of repression converts transient facilitation into long-term functional and structural change. *Cell* **83**, 979–992 (1995).
34. S. Kida, A functional role for CREB as a positive regulator of memory formation and LTP. *Exp. Neurobiol.* **21**, 136–140 (2012).

35. P. M. Quirós *et al.*, Multi-omics analysis identifies ATF4 as a key regulator of the mitochondrial stress response in mammals. *J. Cell Biol.* **216**, 2027–2045 (2017).
36. T. Maier, M. Güell, L. Serrano, Correlation of mRNA and protein in complex biological samples. *FEBS Lett.* **583**, 3966–3973 (2009).
37. R. de Sousa Abreu, L. O. Penalva, E. M. Marcotte, C. Vogel, Global signatures of protein and mRNA expression levels. *Mol. BioSyst.* **5**, 1512–1526 (2009).
38. V. Rizzo *et al.*, Encoding of contextual fear memory requires de novo proteins in the prelimbic cortex. *Biol. Psychiatry: Cogn. Neurosci. Neuroimaging* **2**, 158–169 (2017).
39. L. D. Zorova *et al.*, Mitochondrial membrane potential. *Anal. Biochem.* **552**, 50–59 (2018).
40. S. Cornelia Koeberle *et al.*, Developmental stage-dependent regulation of spine formation by calcium-calmodulin-dependent protein kinase IIα and Rap1. *Sci. Rep.* **7**, 13409 (2017).
41. M. Costa-Mattioli *et al.*, Translational control of hippocampal synaptic plasticity and memory by the eIF2α kinase GCN2. *Nature* **436**, 1166–1170 (2005).
42. E. Stern, A. Chinnakkaruppan, O. David, N. Sonenberg, K. Rosenblum, Blocking the eIF2α kinase (PKR) enhances positive and negative forms of cortex-dependent taste memory. *J. Neurosci.* **33**, 2517–2525 (2013).
43. V. Sharma *et al.*, Local inhibition of PERK enhances memory and reverses age-related deterioration of cognitive and neuronal properties. *J. Neurosci.* **38**, 648–658 (2018).
44. B. Abdulkarim *et al.*, A missense mutation in PPP1R15B causes a syndrome including diabetes, short stature, and microcephaly. *Diabetes* **64**, 3951–3962 (2015).
45. G. Borck *et al.*, eIF2γ mutation that disrupts eIF2 complex integrity links intellectual disability to impaired translation initiation. *Mol. Cell* **48**, 641–646 (2012).
46. M. Skopkova *et al.*, EIF2S3 mutations associated with severe X-linked intellectual disability syndrome MEHMO. *Hum. Mutat.* **38**, 409–425 (2017).
47. S. Moortgat *et al.*, Two novel EIF2S3 mutations associated with syndromic intellectual disability with severe microcephaly, growth retardation, and epilepsy. *Am. J. Med. Genet., Part A* **170**, 2927–2933 (2016).
48. P. J. Zhu *et al.*, Activation of the ISR mediates the behavioral and neurophysiological abnormalities in Down syndrome. *Science* **366**, 843–849 (2019).
49. M. M. Oliveira *et al.*, Correction of eIF2-dependent defects in brain protein synthesis, synaptic plasticity, and memory in mouse models of Alzheimer's disease. *Sci. Signaling* **14**, eabc5429 (2021).
50. X. Tan, S. H. Shi, Neocortical neurogenesis and neuronal migration. *Wiley Interdiscip. Rev. Dev. Biol.* **2**, 443–459 (2013).
51. W. Huang *et al.*, Translational control by eIF2α phosphorylation regulates vulnerability to the synaptic and behavioral effects of cocaine. *eLife* **5**, e12052 (2016).
52. A. N. Placzek *et al.*, eIF2α-mediated translational control regulates the persistence of cocaine-induced LTP in midbrain dopamine neurons. *eLife* **5**, e17517 (2016).
53. R. Kimura *et al.*, Acute exposure to the mitochondrial complex I toxin rotenone impairs synaptic long-term potentiation in rat hippocampal slices. *CNS Neurosci. Ther.* **18**, 641–646 (2012).
54. M. J. Alldred, S. H. Lee, G. E. Stutzmann, S. D. Ginsberg, Oxidative phosphorylation is dysregulated within the basocortical circuit in a 6-month old mouse model of Down syndrome and Alzheimer's disease. *Front. Aging Neurosci.* **13**, 707950 (2021).
55. M. J. Alldred *et al.*, Profiling basal forebrain cholinergic neurons reveals a molecular basis for vulnerability within the Ts65Dn model of Down syndrome and Alzheimer's disease. *Mol. Neurobiol.* **58**, 5141–5162 (2021).
56. S. S. Adav, J. E. Park, S. K. Sze, Quantitative profiling brain proteomes revealed mitochondrial dysfunction in Alzheimer's disease. *Mol. Brain* **12**, 8 (2019).
57. D. Keller, C. Erö, H. Markram, Cell densities in the mouse brain: A systematic review. *Front. Neuroanat.* **12**, 83 (2018).
58. V. Stratoulias *et al.*, ARG1-expressing microglia show a distinct molecular signature and modulate postnatal development and function of the mouse brain. *Nat. Neurosci.* **26**, 1008–1020 (2023).
59. M. Munyeshyaka, R. D. Fields, Oligodendroglia are emerging players in several forms of learning and memory. *Commun. Biol.* **5**, 1148 (2022).
60. R. D'Hooge, P. P. De Deyn, Applications of the Morris water maze in the study of learning and memory. *Brain Res. Rev.* **36**, 60–90 (2001).
61. A. Kumar *et al.*, 2-Deoxyglucose drives plasticity via an adaptive ER stress-ATF4 pathway and elicits stroke recovery and Alzheimer's resilience. *Neuron* **111**, 2831–2846.e2810 (2023).
62. K. Katz *et al.*, The Sequence Read Archive: A decade more of explosive growth. *Nucleic Acids Research* **50**, D387–D390 (2022).